IS THE POMERON NECESSARY AND IF SO WHY IS IT SO COMPLICATED?

Uri Maor

Raymond and Beverly Sackler Faculty of Exact Science

Tel Aviv University, Tel Aviv, 69978, Israel

EDS XIV BLOIS WORKSHOP, December 15-21, 2011. Quy Nhon, Vietnam

Abstract: The elements of the GLM updated Pomeron model are briefly presented and its predictions are compared with the recent soft scattering LHC data. The comparison includes other updated Pomeron models, as well as, a few non Pomeronic calculations.

INTRODUCTION:

The objective of this presentation is to show that the updated Pomeron ($I\!P$) models provide a unique option for a theoretically self consistent unified description of elastic and diffractive soft scattering. In the following I shall present the architecture of the GLM updated $I\!P$ model. It is based on the classical Regge model, taking into account s and t channel unitarity. Its partonic interpretation connects it with the hard pQCD $I\!P$. The model features are compatible with N=4 SYM. A comparison with LHC data and other models will be presented.

THE ARCHITECTURE OF THE UPDATED POMERON MODELS

The simple DL Regge $I\!P$ model with a trajectory

$$\alpha_{I\!P}(t) = 1 + \Delta_{I\!P} + \alpha'_{I\!P} t, \quad \text{where,} \quad \Delta_{I\!P} = 0.08, \alpha'_{I\!P} = 0.25 GeV^{-2},$$

has evolved through the years into a multi-layered construction.

1) A bare non screened $I\!P$ exchange amplitude with $\Delta_{I\!P} > 0$ in a 2x2 Good-Walker (GW) system in which the two eigen states of the soft scattering matrix are super positions of the proton and a "low mass" GW diffactive (with a non specified mass) wave functions.

2) s-channel unitarity screening is initiated by the eikonal model with three input fitted (or tuned) opacities with which we construct the screened and bounded GW amplitudes: $A_{1,1}, A_{2,2}$ and $A_{1,2} = A_{2,1}$. The GW elastic and diffractive SD and DD amplitudes are constructed as linear combinations of the $A_{i,k}$ amplitudes.

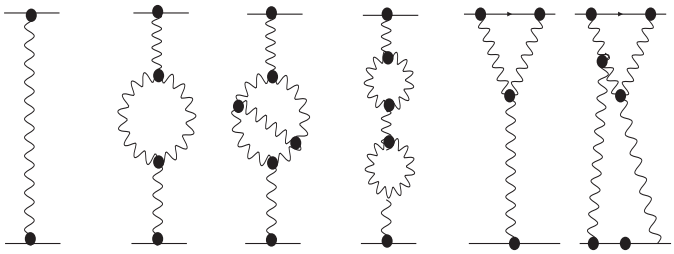

a) *b)*

3) t-channel unitarity is coupled to multi-$I\!P$ interactions, leading to "high mass" non GW SD and DD. Additional screening of the GW and non GW amplitudes is initiated by the screening of $\Delta_{I\!P}$.

4) The survival probability S^2, which has GW and non GW components, initiates further suppression of non GW diffraction (soft or hard).

5) Current $I\!P$ models have an adjusted input of a large $\Delta_{I\!P}$ and a diminishing $\alpha'_{I\!P}$. In the classic Regge model $\Delta_{I\!P}$ controls the energy dependence of the scattering amplitudes, whereas $\alpha'_{I\!P}$ controls the shrinkage of the forward cones. These features are initiated in the updated $I\!P$ models by s and t screenings.

6) The diminishing value of $\alpha'_{I\!P}$ leads to a high p_t partonic interpretation of the $I\!P$ which enables a utilization of pQCD in the summation of the multi $I\!P$ diagrams and a possible BFKL like interpretation of the soft $I\!P$.

7) The adjusted large $\Delta_{I\!P}$ and diminishing $\alpha'_{I\!P}$ are compatible with N=4 SYM.

S-CHANNEL UNITARITY SCREENINGS

Enforcing unitarity is model dependent. In a GW eikonal model the s-channel unitarity equation, $Im\, A_{i,k}\,(s,b) = |A_{i,k}\,(s,b)\,|^2 + G^{in}_{i,k}(s,b)$, is analogous to the single channel equation. $A_{i,k}(s,b) = i(1 - e^{-\frac{\Omega_{i,k}(s,b)}{2}})$ and $G^{in}_{i,k}(s,b) = 1 - e^{-\Omega_{i,k}(s,b)}$, which is the summed probability for all non GW inelastic processes, including non GW "high mass diffraction" induced by multi-$I\!P$ interactions. The opacities, $\Omega_{i,k}(s,b)$, are real, determined by the Born term input.

MULTI-POMERON INTERACTIONS

Mueller applied 3 body unitarity to equate the $a + b \to M + b$ amplitude square with the triple Regge diagram $a + b + \bar{b} \to a + b + \bar{b}$. The core of this representation is a triple vertex with a leading $3I\!P$ term. The equation is valid for "high mass diffraction", where, $\frac{m_p}{M^2} << 1$

and $\frac{M^2}{s} << 1$. Muller's $3I\!P$ approximation is the lowest order of a very large family of multi-$I\!P$ interactions which are not included in the GW mechanism. This dynamical feature is compatible with t-channel unitarity. The figure shows the low order $I\!P$ Green's function.
a) Enhanced diagrams which renormalize the $I\!P$ propagator.
b) Semi-enhanced diagrams which renormalize the p-$I\!P$-p vertexes.
The complexity of the multi-$I\!P$ diagrams results in model dependent summation procedures.

THE PARTONIC POMERON

The microscopic sub structure of the Pomeron is provided by Gribov partonic interpretation of Regge theory, in which the slope of the Pomeron trajectory is related to the mean transverse momentum of the partonic dipoles constructing the Pomeron, and consequently, the running QCD coupling constant: $\alpha'_{I\!P} \propto 1/ < p_t >^2, \quad \alpha_S \propto \pi/ln\left(< p_t^2 > /\Lambda^2_{QCD}\right) << 1$.
Intuitively, these relations suggest a connection between the soft and hard $I\!P$. This is a non trivial connection as the soft $I\!P$ is a simple moving pole in the J-plane, while, the BFKL hard $I\!P$ is a branch cut. Recall, though, that, the BFKL $I\!P$ is commonly approximated as a simple J-pole with $\Delta_{I\!P} = 0.2 - 0.3$ and $\alpha'_{I\!P} = 0$
Following I shall discuss 4 $I\!P$ models. The models are conceptually similar, but differ in their $I\!P$ features.
GLM (Tel AVIV): have a single $I\!P$, $\Delta_{I\!P} = 0.20$, $\alpha'_{I\!P} \simeq 0$.
KMR (Durham) have: $\Delta_{I\!P} = 0.3$, $\alpha'_{I\!P} \propto 1/p_t^2$.
Ostapchenko (Bergen): has 2 Pomerons, soft: $\Delta_{I\!P} = 0.17$, $\alpha'_{I\!P} = 0.11$,
and hard: $\Delta_{I\!P} = 0.31$, $\alpha'_{I\!P} = 0.085$.
Kaidalov-Poghosyan (Moscow): is a single channel $I\!P$ model with (many!) secondary Regge trajectories, $\Delta_{I\!P} = 0.12$, $\alpha'_{I\!P} = 0.22$.
Note that, in GLM the hardness of the single $I\!P$ is determined by the strength of the unitarity screenings. In the extreme, non screened $I\!P$ is hard and when strongly screened it is soft. This picture is supported by HERA e-p DIS. In KMR the hardness is explicitly determined by p_t^2. Kaidalov-Poghosyan is a soft $I\!P$ model.
A critical difference between GLM and the other listed $I\!P$ models relates to the calculation of a multi $I\!P$ vertex. GLM utilize pQCD procedures, where $nI\!P \to mI\!P$ reduces to a sequence of $G_{3I\!P}$ vertexes. $G_{3I\!P}$ is a free parameter, so is $\gamma^2 = \int G_{3I\!P} d^2p_t$.
KMR couplings are $g_m^n = \frac{1}{2}\, g_N\, nm\, \lambda^{n+m-2} = \frac{1}{2}\, nm\, G_{3I\!P}\, \lambda^{n+m-3}$. λ is a free parameter,

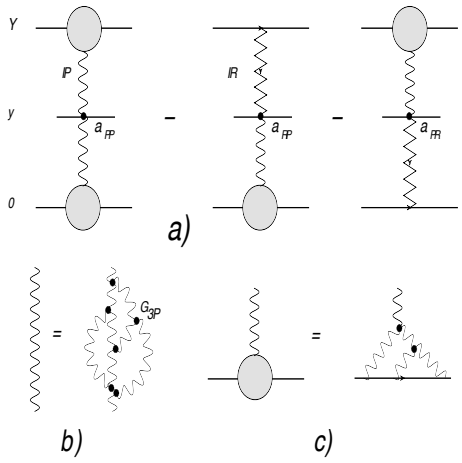

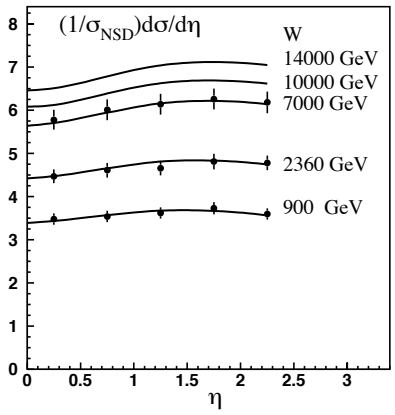

$n + m > 2$, $G_{3I\!P} = \lambda g_N$. Kaidalov and Ostapchenko have the same expression with a different normalization.

LHC CROSS SECTION DATA

1) NSD data on $dN_{ch}/d\eta = \{1/\sigma_{NSD}\}d\sigma/d\eta$, the charged multiplicity density distribution, has been published by ALICE, CMS and ATLAS at central pseudo rapidity $-2.5 \leq \eta \leq 2.5$. This data provides an additional perspective on the $I\!P$ model. In the framework of Gribov's $I\!P$ calculus. Single inclusive cross sections can be calculated using Mueller diagrams. To this end we have utilized the fitted parameters of the GLM $I\!P$ model. We add 3 phenomenological parameters: $a_{I\!P I\!P}$ and $a_{I\!P R} = a_{R I\!P}$, which account for hadron emission from the exchanged $I\!P$ or Reggeon. Q is the average transverse momentum of the produced mini-jets. The complete data base for this fit is obtained from experiments spread over many years with different approaches to their data analysis. We have fitted first the 546, 900, 1800, 2360, 7000 GeV data. The second fit was confined to the very recent CMS data at 900, 2360, 7000

ATLAS	ALICE	CMS	TOTEM
$69.4 \pm 2.4 \pm 6.9$	$72.7 \pm 1.1 \pm 5.1$	$71.8 \pm 1.1 \pm 2.0 \pm 7.9$	$73.5 \pm 0.6 + 1.8 - 1.3$

TABLE I: LHC σ_{inel} at 7 TeV

Achilli et al.	Block-Halzen	GLM	Kaidalov-Poghosyan	KMR
60-75	69.0	72.2	70.0	62.6-67.1

TABLE II: σ_{inel} model predictions at 7 TeV

GeV. The two sets of fitted parameters are compatible. The figure shows our fit of the CMS distributions. These results are significant, as they provide a consistent reproduction of the SppS-Tevatron-LHC inclusive data.

2) $\sigma_{inel} = \sigma_{tot} - \sigma_{el} = \sigma_{sd} + \sigma_{dd} + \sigma_{nd}$. The first LHC measurements of the inelastic cross section were derived from the minimum bias data samples. The 2 tables above compare the 7 TeV σ_{inel} data and its model predictions.

3) TOTEM recently published their preliminary results at 7 TeV, $\sigma_{tot} = 98.3 \pm 2.71 mb$ and $\sigma_{el} = 24.8 \pm 2.81$. The table below presents the corresponding model predictions. As seen, the theoretical predictions are moderately below the TOTEM data.

$I\!P$ models' problem is that their formalism has a large number of free parameters, in no proportion to their small adjusted data base. In my opinion, prior to theoretical modifications, one should improve the adjustment procedures.

As it stands, the predictions of Halzen-Igi are some what better than the competition. However, this class of models has two deficiencies:

i) It is a phenomenological parton model based mostly on successful parametrizations.

ii) It does not incorporate diffraction with elastic scattering.

	Achilli et al.	Block-Halzen	Halzen-Igi et al.	GLM	KP	KMR
σ_{tot}mb	91.6	95.4	96.1	94.2	96.4	89.0
σ_{el} mb		26.4		22.9	24.8	21.9

TABLE III: σ_{tot} and σ_{el} theoretical predictions.

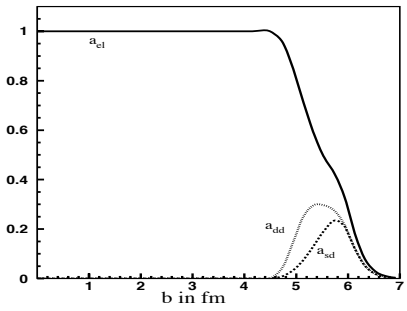

EXCEEDINGLY HIGH ENERGY BEHAVIOR

The definitions of GW and non GW diffraction have profound implication on the exceedingly high energy approach toward the black disc bound.

Single channel models neglect the GW mixing of the proton and "low mass" diffractive wave functions. In a single channel non GW model, $\sigma_{el} \leq \frac{1}{2}\sigma_{tot}$ and $\sigma_{inel} \geq \frac{1}{2}\sigma_{tot}$. Equality is reached at the saturated black disc bound, where $\sigma_{el} = \sigma_{inel} = \frac{1}{2}\sigma_{tot}$.

In GW multi-channel models we distinguish between GW and non GW diffraction. Assuming a multi channel eikonal model we obtain the Pumplin bound: $(\sigma_{el} + \sigma^{GW}_{diff}) \leq \frac{1}{2}\sigma_{tot}$. Equality is attained at the black disc saturation. The implication is that in a multi-channel GW model, $\quad \sigma_{el} \leq \frac{1}{2}\sigma_{tot} - \sigma^{GW}_{diff}, \quad \sigma_{inel} \geq \frac{1}{2}\sigma_{tot} + \sigma^{GW}_{diff}$.

In a recent publication, Block and Halzen analyzed an AUGER event for which they obtain at $W = 57 \pm 6TeV : \sigma_{tot} = 134.8mb$ and $\sigma_{inel} = 90mb$. i.e. $\frac{\sigma_{inel}}{\sigma_{tot}} = 0.67$. The corresponding GLM predictions are: $\sigma_{tot} = 122mb$, $\sigma_{el} = 31.1mb. \sigma_{inel} = 90.9$, $\sigma_{sd} = 21mb\, \sigma_{dd} = 13.5mb$, i.e. $\frac{\sigma_{inel}}{\sigma_{tot}} = 0.75$. The implication from those very different models is that s-channel saturation will be attained, if at all, at energies of the order of the Planck scale.

The basic GW amplitudes are $A_{1,1}$, $A_{1,2}$ and $A_{2,2}$. These are the building blocks with which we construct a_{el}, a_{sd} and a_{dd}. The $A_{i,k}$ amplitudes are bounded by the unitarity black disc bound of unity. $a_{el}(s,b)$ reaches this bound at a given (s,b) when, and only when, $A_{1,1}(s,b) = A_{1,2}(s,b) = A_{2,2}(s,b) = 1$, independent of the value of the GW mixing parameter. Consequently, when $a_{el}(s,b) = 1$, $a_{sd}(s,b) = a_{dd}(s,b) = 0$.

Lets re-check the diffractive channels at exceedingly high energies. The elastic amplitude which is essentially black, has a high b tail where $a_{el}(s,b) < 1$. In this domain diffraction can survive. The Figure shows the GLM elastic, SD and DD amplitudes at the Planck scale.